Anti-inflammatory function of high-density lipoproteins via autophagy of I B Kinase

Gerster, Ragam ; Eloranta, Jyrki J ; Hausmann, Martin ; Ruiz, Pedro A ; Cosin-Roger, Jesus ; Terhalle, Anne ; Ziegler, Urs ; Kullak-Ublick, Gerd A ; von Eckardstein, Arnold ; Rogler, Gerhard

Abstract: Background Aims: Plasma levels of high-density lipoprotein (HDL) cholesterol are frequently found decreased in patients with inflammatory bowel disease (IBD). Therefore, and because HDL exerts anti-inflammatory activities, we investigated whether HDL and its major protein component apolipoprotein A-I (apoA-I) modulate mucosal inflammatory responses in vitro and in vivo. Methods: The human intestinal epithelial cell line T84 was used as the in vitro model for measuring the effects of HDL on the expression and secretion of tumor necrosis factor (TNF), interleukin-8 (IL-8), and intracellular adhesion molecule (ICAM). Nuclear factor- B (NF- B)-responsive promoter activity was studied by dual luciferase reporter assays. Mucosal damage from colitis induced by dextran sodium sulphate (DSS) and 2,4,6-trinitrobenzenesulfonic acid (TNBS) was scored by colonoscopy and histology in apoA-I transgenic (Tg) and apoA-I knockout (KO) and wild-type (WT) mice. Myeloperoxidase (MPO) activity and TNF and ICAM expression were determined in intestinal tissue samples. Autophagy was studied by Western blot analysis, immunofluorescence, and electron microscopy. Results: HDL and apoA-I down-regulated TNF-induced mRNA expression of TNF, IL-8, and ICAM, as well as TNF-induced NF- B-responsive promoter activity. DSS/TNBS-treated apoA-I KO mice displayed increased mucosal damage upon both colonoscopy and histology, increased intestinal MPO activity and mRNA expression of TNF and ICAM as compared with WT and apoA-I Tg mice. In contrast, apoA-I Tg mice showed less severe symptoms monitored by colonoscopy and MPO activity in both the DSS and TNBS colitis models. In addition, HDL induced autophagy, leading to recruitment of phosphorylated I B kinase to the autophagosome compartment, thereby preventing NF- B activation and induction of cytokine expression. Conclusions: Taken together, the in vitro and in vivo findings suggest that HDL and apoA-I suppress intestinal inflammation via autophagy and are potential therapeutic targets for the treatment of IBD.

DOI: https://doi.org/10.1016/j.jcmgh.2014.12.006

Gerster, Ragam; Eloranta, Jyrki J; Hausmann, Martin; Ruiz, Pedro A; Cosin-Roger, Jesus; Terhalle, Anne; Ziegler, Urs; Kullak-Ublick, Gerd A; von Eckardstein, Arnold; Rogler, Gerhard (2015). Anti-inflammatory function of high-density lipoproteins via autophagy of I B Kinase. Cellular and Molecular Gastroenterology and Hepatology, 1(2):171-187.e1.
DOI: https://doi.org/10.1016/j.jcmgh.2014.12.006

cmgh
CELLULAR AND MOLECULAR GASTROENTEROLOGY AND HEPATOLOGY

ORIGINAL RESEARCH

Anti-inflammatory Function of High-Density Lipoproteins via Autophagy of IκB Kinase

Ragam Gerster,[1,2,3] Jyrki J. Eloranta,[2] Martin Hausmann,[1] Pedro A. Ruiz,[1] Jesus Cosin-Roger,[1,4] Anne Terhalle,[1] Urs Ziegler,[5] Gerd A. Kullak-Ublick,[2,3] Arnold von Eckardstein,[3,6] and Gerhard Rogler[1,3]

[1]*Division of Gastroenterology and Hepatology, University Hospital Zurich, Zurich, Switzerland;* [2]*Department of Clinical Pharmacology and Toxicology, University Hospital Zurich, Schlieren, Switzerland;* [3]*Zurich Center of Integrative Human Physiology, University of Zurich, Zurich, Switzerland;* [4]*Departamento de Farmacología and CIBERehd, Facultad de Medicina, Universidad de Valencia, Valencia, Spain;* [5]*Centre for Microscopy and Image Analysis, University Hospital Zurich, Zurich, Switzerland;* [6]*Institute of Clinical Chemistry, University Hospital Zurich, Zurich, Switzerland*

SUMMARY

High-density lipoprotein and its major protein constituent apolipoprotein A-I suppress intestinal inflammation in vitro and in vivo via activation of the autophagic pathway.

BACKGROUND & AIMS: Plasma levels of high-density lipoprotein (HDL) cholesterol are frequently found decreased in patients with inflammatory bowel disease (IBD). Therefore, and because HDL exerts anti-inflammatory activities, we investigated whether HDL and its major protein component apolipoprotein A-I (apoA-I) modulate mucosal inflammatory responses in vitro and in vivo.

METHODS: The human intestinal epithelial cell line T84 was used as the in vitro model for measuring the effects of HDL on the expression and secretion of tumor necrosis factor (TNF), interleukin-8 (IL-8), and intracellular adhesion molecule (ICAM). Nuclear factor-κB (NF-κB)-responsive promoter activity was studied by dual luciferase reporter assays. Mucosal damage from colitis induced by dextran sodium sulphate (DSS) and 2,4,6-trinitrobenzenesulfonic acid (TNBS) was scored by colonoscopy and histology in apoA-I transgenic (Tg) and apoA-I knockout (KO) and wild-type (WT) mice. Myeloperoxidase (MPO) activity and TNF and ICAM expression were determined in intestinal tissue samples. Autophagy was studied by Western blot analysis, immunofluorescence, and electron microscopy.

RESULTS: HDL and apoA-I down-regulated TNF-induced mRNA expression of TNF, IL-8, and ICAM, as well as TNF-induced NF-κB-responsive promoter activity. DSS/TNBS-treated apoA-I KO mice displayed increased mucosal damage upon both colonoscopy and histology, increased intestinal MPO activity and mRNA expression of TNF and ICAM as compared with WT and apoA-I Tg mice. In contrast, apoA-I Tg mice showed less severe symptoms monitored by colonoscopy and MPO activity in both the DSS and TNBS colitis models. In addition, HDL induced autophagy, leading to recruitment of phosphorylated IκB kinase to the autophagosome compartment, thereby preventing NF-κB activation and induction of cytokine expression.

CONCLUSIONS: Taken together, the in vitro and in vivo findings suggest that HDL and apoA-I suppress intestinal inflammation via autophagy and are potential therapeutic targets for the treatment of IBD. *(Cell Mol Gastroenterol Hepatol 2015; 1:171–187; http://dx.doi.org/10.1016/j.jcmgh.2014.12.006)*

Keywords: Apolipoprotein A-I; Autophagy; Inflammatory Bowel Disease; NF-κB.

High-density lipoproteins (HDL) are particles composed of proteins and lipids synthesized by the liver and the intestine. In addition to mediating reverse transport of cholesterol from macrophages to the liver,[1–4] HDL performs many anti-inflammatory activities.[5–7] Whereas the reverse cholesterol transport-function of HDL has become the classic explanation for the inverse association between HDL cholesterol levels and cardiovascular risk, both the mechanisms and the consequences of its anti-inflammatory properties are less well understood. In an in vivo model of intestinal inflammation, colonoscopy and histology showed increased mucosal damage and inflammation in apolipoprotein A-I (apoA-I) knockout (KO) mice, which lack HDL. In contrast, transgenic (Tg) mice overexpressing human apoA-I, which has very high plasma levels of HDL, were protected from intestinal inflammation. In cultivated enterocytes, both HDL and its major protein component apoA-I down-regulated the expression of proinflammatory cytokines in vitro via a nuclear factor-κB

Abbreviations used in this paper: **ApoA-I, apolipoprotein A-I; CD, Crohn's disease; DAPI, 4′,6-diamidino-2-phenylindole; DSS, dextran sodium sulphate; EMSA, electrophoretic mobility shift assay; HDL, high-density lipoprotein; IBD, inflammatory bowel disease; ICAM, intracellular adhesion molecule; IL, interleukin; KO, knockout; LC3II, light chain 3 II; 3-MA, 3-methyl adenine; MEICS, murine endoscopic index of colitis severity; MPO, myeloperoxidase; mTOR, the mammalian target of rapamycin; NF-κB, nuclear factor κB; PBS, phosphate-buffered saline; PFA, paraformaldehyde; PI-3, phosphatidylinositol-3; p-IKK, phosphorylated IκB kinase; RT-PCR, real-time polymerase chain reaction; siRNA, small interfering RNA; Tg, transgenic; TNBS, 2,4,6-trinitrobenzenesulfonic acid; TNF, tumor necrosis factor; WT, wild type.**

2352-345X
http://dx.doi.org/10.1016/j.jcmgh.2014.12.006

(NF-κB)-dependent pathway. In addition, HDL stimulated the expression of light chain 3 II (LC3II), an autophagosomal membrane-bound protein, through the inhibition of mTOR, the mammalian target of rapamycin, and induced autophagy. HDL-induced autophagy led to the recruitment of phosphorylated IκB kinase (p-IKK, which mediates NF-κB activation) to the autophagosome compartment, thereby preventing further NF-κB activation and induction of cytokine expression. Inhibition of autophagy reversed the suppressive effect of HDL on inflammation. Thus, HDL and its major protein component apolipoprotein A-I (apoA-I) act in an anti-inflammatory manner via induction of autophagy and subsequent recruitment of p-IKK to the autophagosome compartment. The clinical exploitation of HDL could be significant for the treatment of inflammatory diseases such as inflammatory bowel disease (IBD).

HDL encompasses a heterogeneous class of plasma lipoproteins, which contain apoA-I as the main protein, and phospholipids and cholesterol as the main lipids. HDL particles as well as apoA-I exert various anti-inflammatory, antioxidative, and cytoprotective effects in vitro and in vivo, which are thought to confer protection against chronic inflammatory disorders.[8,9] A low plasma concentration of HDL cholesterol is a risk factor for cardiovascular disease, diabetes mellitus, and certain cancers.[10–15]

The intestine and liver are the major organs responsible for HDL synthesis. Dysfunction of either of these organs as a result of inflammation is associated with a decrease in plasma levels of HDL cholesterol and apoA-I.[16,17] For example, HDL cholesterol levels are significantly decreased in patients with active IBD.[18,19] Traditionally, it was thought that low levels of HDL cholesterol in IBD patients are a consequence of the disorder; however, due to the well-known anti-inflammatory effects of HDL, we hypothesized that HDL and apoA-I might in fact modulate intestinal inflammation in such patients. Having established the anti-inflammatory effects of HDL and apoA-I in the intestine, we further hypothesized that autophagy plays a role in this process as earlier studies had shown an uptake of HDL into intracellular compartments now identified as autophagosomes.[20]

Materials and Methods

Cell Cultures

Human colon-derived epithelial cell line T84 cells were cultured in Dulbecco's modified Eagle's medium 12 (Invitrogen, Basel, Switzerland) in a humidified atmosphere containing 5% CO_2 at 37°C. The medium was supplemented with 10% fetal bovine serum (Bruschwig, Basel, Switzerland) and penicillin/streptomycin (100 μg/mL/100 μg/mL) (Invitrogen).

Isolation of High-Density Lipoprotein and Apolipoprotein A-I from Plasma

Human HDL ($1.063<d<1.21$ kg/L) was isolated from the plasma of normolipidemic blood donors by sequential ultracentrifugation.[21] Purity was confirmed using sodium dodecyl sulfate polyacrylamide gel electrophoresis and by the presence of apoA-I and the absence of low-density lipoprotein, apolipoprotein B, and albumin. ApoA-I was purified from delipidated HDL by fast protein liquid chromatography.[22]

RNA Isolation, Reverse Transcription, and Real-Time Polymerase Chain Reaction

The T84 cells were incubated with HDL 50–200 μg/mL for 18 hours and then with tumor necrosis factor (TNF) 25 ng/mL for 3 hours. Total RNA was isolated using TRIzol reagent (Invitrogen). We reverse transcribed 1–2 μg RNA with a High-Capacity cDNA Reverse Transcription Kit (Applied Biosystems, Rotkreuz, Switzerland) before real-time polymerase chain reaction (RT-PCR) analysis (7900HT; Applied Biosystems) using various TaqMan assays: Hs00174128_m1 (human TNF), Mm00443258_m1 (murine TNF), Hs00174103_m1 (human interleukin-8 [IL-8]), Hs00164932_m1 (human intracellular adhesion molecule [ICAM]), Mm00516023_m1 (murine ICAM), Hs00222677_m1 (human β-actin), 4352341E_mACTB (murine β-actin), Hs00797944_s1 (LC3), Hs00250530_m1 (ATG16L1), and endogenous controls for human and animals (Applied Biosystems). Constitutively expressed β-actin was measured as an internal standard for normalization. Relative mRNA levels were calculated using the comparative threshold cycle method. For each experiment, all tests were performed in triplicate. The mRNA levels obtained in control conditions were set to 1, and the results are shown relative to those.

Luciferase Reporter Assays

Cells were cotransfected with the luciferase reporter constructs of NF-κB (400 ng) and the expression plasmids pTAL-luc (200 ng) at a ratio of 3 μg FuGENE HD per 1 μg DNA. The pcDNA33.1(+) vector was added to normalize the amount of DNA transfected, where necessary. We cotransfected 100 ng of the *Renilla* luciferase (pRL-CMV) reporter plasmid (Promega, Dübendorf, Switzerland) to assess transfection efficiency. Cells were harvested 36 hours after transfection, and luciferase activity was determined using the Dual Luciferase Assay System (Promega) and a Luminoskan Ascent Microplate Luminometer (Thermo Fisher Scientific, Wohlen, Switzerland). Reporter activities obtained from the empty pGL3basic corresponding to each test condition and for the test construct containing the test promoter in the control conditions were set to 1, and fold activities were shown relative to this. All experiments were performed in triplicate and repeated at least three times.

Electrophoretic Mobility Shift Assays

Oligonucleotides with 5-GATC overhangs were used for annealing NF-κB consensus (top strand, 5-GATCAGTT GAGGGGACTTTCCCAGGC-3; bottom strand, 5-GATCGCCTGG GAAAGTCCCCTCAACT) for radioactive labeling by fill-in reactions as described by Saborowski et al.[23] Protein (5 μg) from nuclear extracts prepared by using the NE-PER extraction kit (Pierce, Lausanne, Switzerland) were mixed with 50,000 cpm (1.0 ng) of the radioactive probe, and

protein-DNA complexes were allowed to form for 30 minutes at 30°C. In supershift experiments, 1 μg of the anti-NF-κB p65 antibody (C-20; Santa Cruz Biotechnology, Santa Cruz, CA) was added to the extracts before binding reactions and incubated at 4°C for 1 hour before the addition of radioprobes. The electrophoretic mobility shift assay (EMSA) gels were run at 200V in 0.5X Tris-borate-ethylene-diamine-tetraacetic acid (EDTA) and processed as described for autoradiography.[23]

Animals

Female wild-type (WT) (C57BL/6J) mice, apoA-I knockout (KO) (B6.129P2-ApoA-Itm1Unc/J [−/−]) mice, and apoA-I Tg (C57BL/6-Tg [ApoA-I]1Rub/J) mice (all 7–8 weeks old) were used. The animals, which were purchased from the Jackson Laboratory (Bar Harbor, ME), were housed in a specified pathogen-free facility in individually ventilated cages. For the dextran sodium sulphate (DSS) model, colitis was induced with drinking water containing 2.5% of DSS (MP Biomedicals, Illkirch, France).[24] The animals were divided into six groups: three DSS groups and three DSS-free water control groups (with six mice in each group). Animals were fed food and water with or without DSS ad libitum; 24 hours before animals were sacrificed, DSS groups were fed with water without DSS.

For the 2,4,6-trinitrobenzenesulfonic acid (TNBS) model, colitis was induced with TNBS (Fluka/Sigma-Aldrich Chemie Gmbh, Munich, Germany) with five mice in each group. Briefly, on day 1, mice were shaved between the shoulders, and 150 μL of TNBS presensitization solution (final concentration 1% in ethanol/acetone/olive oil) was applied to the abdominal skin. On day 8, 100 μL of TNBS solution (final concentration 2.5% in 50% ethanol) was slowly administered into the colon 4 cm proximal to the anus with a 3.5F catheter to a 1 ml syringe. The catheter was gently removed from the colon, and the mouse was kept with the head down in a vertical position for 60 seconds. Mice were sacrificed on day 18.[25] All the animal experiments were approved by the veterinary authorities of Zurich, Switzerland, and were performed according to Swiss animal welfare laws.

Determination of Colonoscopy and Total Histologic Score

Macroscopic mucosal damage was assessed by colonoscopy scoring using the murine endoscopic index of colitis severity (MEICS), monitored by a miniendoscope. Animals were anesthetized intraperitoneally with a mixture of ketamine, 90–120 mg/kg body weight (Vétoquinol, Bern, Switzerland), and xylazine, 8 mg/kg body weight (Bayer, Lyssach, Switzerland), and were examined as described previously elsewhere.[26–28] The endoscope was introduced with a lubricant (2% lidocaine) through the anus in the sedated mouse, the colon was gently inflated with air, and photographs were taken. Recording was performed with the Karl Storz Tele Pack Pal 20043020 (Karl Storz Endoskope, Tuttlingen, Germany).

The MEICS was scored based on mucosal bleeding, abundant fibrin, altered vascular pattern, nontransparent mucosa (granularity), and stool composition as described by Becker et al.[26] Colonoscopy was performed on day 8 before sacrificing the mice. From the distal third of the colon, 1 cm of colonic tissue was removed, washed with saline buffer, and fixed in 4% formalin overnight. Sections of the paraffin-embedded tissue were used for histologic analysis, as described previously elsewhere, based on loss of crypts, loss of goblet cells, infiltration of lymphocytes, and thickening of submucosa/mucosa.[25,26] The histologic examination was performed by two independent, blinded investigators.

Isolation and Culture of Human Colonic Lamina Propria Fibroblasts

Primary human colonic lamina propria fibroblast cultures were derived from surgical specimens of patients with active Crohn's disease and were cultured as described previously elsewhere.[29] Fibroblasts were cultured in Dulbecco's modified Eagle's medium containing 10% fetal calf serum, penicillin 100 IU/mL, streptomycin 100 μg/mL, ciprofloxacin 8 μg/mL, gentamicin 50 μg/mL, and amphotericin B 1 μg/mL. Genomic DNA was isolated from cultured fibroblasts and genotyped for the ATG16L1 variant using predesigned genotyping assays (Applied Biosystems, Foster City, CA) and TaqMan technology. Written informed consent was obtained before specimen collection, and the studies were approved by the local ethics committee.

Gold Labeling of High-Density Lipoprotein

Colloidal gold was prepared as described previously elsewhere[30] using a particle size of 8 nm. For the conjugation of HDL to colloidal gold, 10 mL of a monodisperse gold solution was added to a 16-μL lipoprotein solution containing 50 mg of lipoprotein per milliliter in a phosphate buffer at pH 5.5. Excess lipoprotein was removed by centrifugation at 9000 *g* for 20 minutes against glycerine and then dialyzed in Tris-borate-ethylene-diamine-tetraacetic acid (EDTA) buffer to remove the glycerine.

To follow the uptake of HDL into the intestinal cell line, colon carcinoma HT29 cells were incubated with gold-labeled HDL for 18 hours. The cells were washed in phosphate-buffered saline (PBS) and fixed with 2.5% glutaraldehyde + 0.8% formaldehyde in NaCL 50 mM and phosphate buffer 0.1 M for 2 hours at room temperature, postfixed in 1% OsO_4 (phosphate buffer 50 mM) at 4°C for 1 hour, and block stained with 1% uranyl acetate in water for 1 hour. Thereafter, the tissue was dehydrated in ethanol (70%–100%, 30 minutes) and propylene oxide (two times 20 minutes), polymerized, and embedded in Epon Araldite. Electron microscopy was performed on a Philips CM100 transmission electron microscope (Philips, Eindhoven, the Netherlands).

Transfection of Cells with Small Interfering RNAs

Cells were seeded at a density of 400,000 cells/well onto 24-well plates and transfected with LC3 siGenome SMARTpool (Dharmacon, Lafayette, CO) or siCONTROL

nontargeting small interfering RNA (siRNA) #2 (Dharmacon) at a final concentration of 50 nM using the TransIT-TKO reagent (Mirus Bio LLC, Madison, WI). The transfections were repeated after 24 hours, and the cells were harvested in 1 mL TRIzol (Invitrogen) 24 hours after the second transfection.

Western Blotting

Cells were grown on six-well plates for 24 hours, followed by incubation with HDL for 18 hours before treatment with 25 ng/mL TNF for 3 hours where indicated. Cells were harvested into radioimmune precipitation assay buffer with protease inhibitors. The cell debris was removed by centrifugation, and the supernatants were denatured at 94°C. We subjected 20 μg of protein to electrophoresis, which was then blotted onto a nitrocellulose membrane. Immunodetection was performed using anti-phospho-IKKα, anti-phospho mTOR, anti-mTOR (all from Cell Signaling Technology, Beverly, MA), anti-LC3 (Sigma-Aldrich, St. Louis, MO), and anti-actin (Millipore, Billerica, MA) where indicated. The bands were visualized using the electrochemiluminescence system, and densitometry of bands was measured using ImageJ (http://imagej.nih.gov/ij/).

Confocal Microscopy

After treatment of cells with HDL for 18 hours and TNF for 3 hours, the cells were washed with PBS and fixed with 4% paraformaldehyde (PFA) for 15 minutes. For LC3 staining, fixed cells were washed with PBS, permeabilized in 100% methanol at −20°C for 10 minutes, washed with PBS, and blocked with 3% bovine serum albumin for 1 hour at room temperature. Cells were subsequently incubated with LC3/p-IKK antibody (1:200 dilution; Cell Signaling Technology) overnight at 4°C. After 3 PBS-Tween washes, cells were incubated with Alexa 488 conjugated secondary rabbit antibody (Invitrogen) for 1 hour at room temperature and then washed three times in Tris-buffered saline with Tween before mounting with antifade medium (Dako, Glostrup, Denmark). Cells were analyzed by confocal microscopy in a Leica SP5 laser scanning confocal microscope (Leica Microsystems, Wetzlar, Germany) using a Zeiss AxioCam HRm CCD camera, and Zeiss EC Plan-Neofluar 10×/0.3 and Zeiss LD Plan-Neofluar 20×/0.4 objectives (Carl Zeiss Microscopy GmbH, Jena, Germany). After sequential excitation, green and blue fluorescent images of the same sample were acquired and processed using Leica confocal software (LAS-AF Lite; Leica Microsystems).

Results

Anti-inflammatory Effect of High-Density Lipoprotein and Apolipoprotein A-I In Vivo

Intestinal Inflammation Is Ameliorated in Apolipoprotein A-I Transgenic Mice with Dextran Sodium Sulphate Colitis. Upon application of DSS to the drinking water of WT, apoA-I KO, and human apoA-I Tg mice, animals experienced mucosal damage of the intestine and colon but of different severity. The apoA-I Tg mice, which have strongly elevated plasma levels of HDL cholesterol, displayed an intact epithelial surface with still-formed stools compared with the WT mice. In contrast, a severe disruption of the epithelium was observed in the apoA-I KO mice (Figure 1*A*), which are HDL deficient. A histologic analysis of distal colon tissue samples showed that, upon DSS treatment, the apoA-I KO mice had severe barrier breakdown with extensive infiltration reaching the lamina muscularis mucosae, and the total histologic score was significantly increased for apoA-I KO mice (Figure 1*B*).

Weight loss was monitored during the 7-day course of acute colitis. Upon treatment with DSS and in comparison with the DSS-free-water control animals, the body weight decreased significantly in the WT mice and apoA-I KO mice but not in the apoA-I Tg mice (Figure 1*C*). Tissue homogenates of DSS-treated apoA-I Tg mice showed significantly lower myeloperoxidase (MPO) activity than the DSS-treated apoA-I KO mice and WT mice (Figure 1*D*). Finally, DSS supplementation led to a significant increase in mRNA expression of TNF and ICAM in the whole colon tissue in all animals, but the expression of TNF and ICAM in apoA-I KO mice was 18 and 34 times higher, respectively, than in the WT mice, and 10 and 168 times higher, respectively, than in the apoA-I Tg mice (Figure 1*E*).

Intestinal Inflammation Is Ameliorated in Apolipoprotein A-I Transgenic Mice with 2,4,6-Trinitrobenzenesulfonic Acid Colitis. Upon administration of TNBS to the WT, apoA-I KO, and human apoA-I Tg mice, the animals experienced mucosal damage of the intestine and colon but of different severity. Upon TNBS-induced colitis, weight loss in the apoA-I KO mice was significantly higher as compared with the apoA-I Tg mice during the last 2 days before the animals were sacrificed (Figure 2*A*). The macroscopic mucosal damage was assessed by colonoscopy and MEICS. On day 2 after TNBS administration into the colon mucosa, the apoA-I Tg mice displayed a smooth and transparent mucosa with a normal vascular pattern compared with the opaque mucosa with altered vascular pattern in the apoA-I KO mice. On day 9 after TNBS administration, the colon of the apoA-I Tg mice appeared to be less transparent. In the apoA-I KO mice, the colon appeared with a thickened, more granular mucosa and a clearly altered vascular pattern. The apoA-I KO animals were given a significantly higher MEICS score compared with the apoA-I Tg mice (Figure 2*B*). Also on a microscopic level for the apoA-I KO mice, a more severe colitis was found compared with the apoA-I Tg mice. The total histologic score for the apoA-I KO mice with induced TNBS colitis was increased compared with the apoA-I Tg mice (Figure 2*C*).

Anti-inflammatory Effect of High-Density Lipoprotein and Apolipoprotein A-I in Vitro

A series of in vitro experiments in the colonic epithelial cell line T84 were performed to further elucidate the mechanism of the effects found in vivo. These experiments

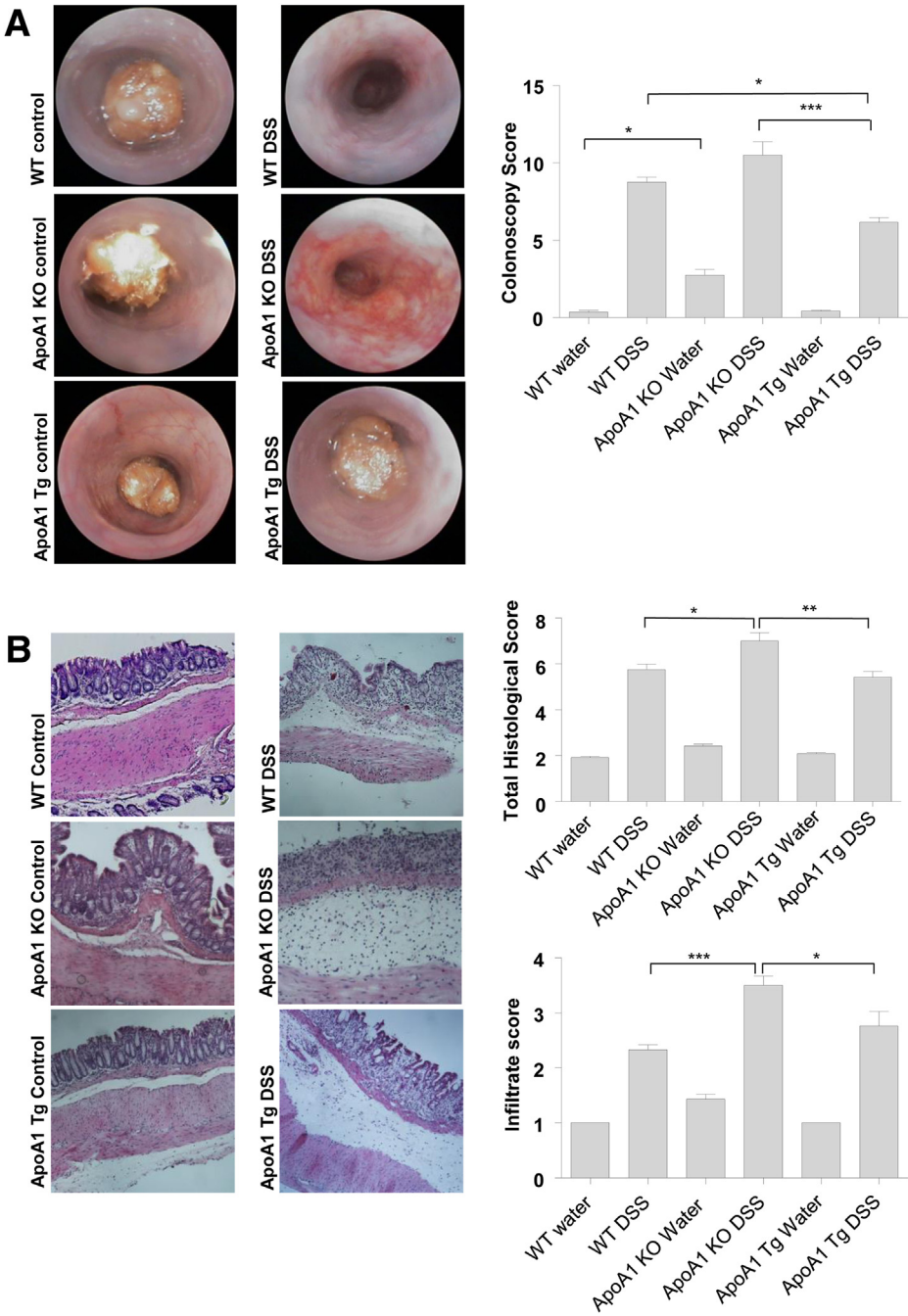

Figure 1. Intestinal inflammation is ameliorated in apolipoprotein A-I transgenic (apoA-I Tg) mice upon colitis induced with dextran sodium sulphate (DSS). (*A*) Miniendoscopy showed severe disruption of the epithelium in apoA-I knockout (KO) mice receiving DSS. Macroscopic mucosal damage was assessed by colonoscopy scoring (murine endoscopic index of colitis severity). Each bar represents the mean ± standard error of the mean (SEM); n = 6; *$P < .05$, ***$P < .001$. (*B*) H&E staining of sections from apoA-I KO mice receiving DSS displayed severe barrier breakdown with extensive infiltration reaching the lamina muscularis mucosae. The total histologic score, calculated as the sum of the epithelium and infiltrate score, was plotted. Each bar represents the mean ± SEM; n = 6; *$P < .05$, **$P < .01$. (*C*) Weight loss was monitored during the 7-day course of acute colitis. Upon treatment with DSS and in comparison with the DSS-free-water control animals, the body weight decreased significantly in wild-type (WT) and apoA-I KO mice ($P < .001$) but not in apoA-I Tg mice. (*D*) Tissue homogenates of DSS-treated apoA-I Tg mice showed significantly lower myeloperoxidase (MPO) activity than the DSS-treated apoA-I KO and WT mice ***$P < .001$. (*E*) Upon DSS-induced colitis, apoA-I KO mice receiving DSS displayed a significant increase in mRNA expression of tumor necrosis factor (TNF) and intracellular adhesion molecule (ICAM), whereas apoA-I Tg mice displayed lower expression levels of TNF and ICAM compared with WT and apoA-I KO mice. The mRNA expression was calculated relative to WT mice receiving DSS-free water. Each bar represents the mean ± SEM; n = 6; ***$P < .001$).

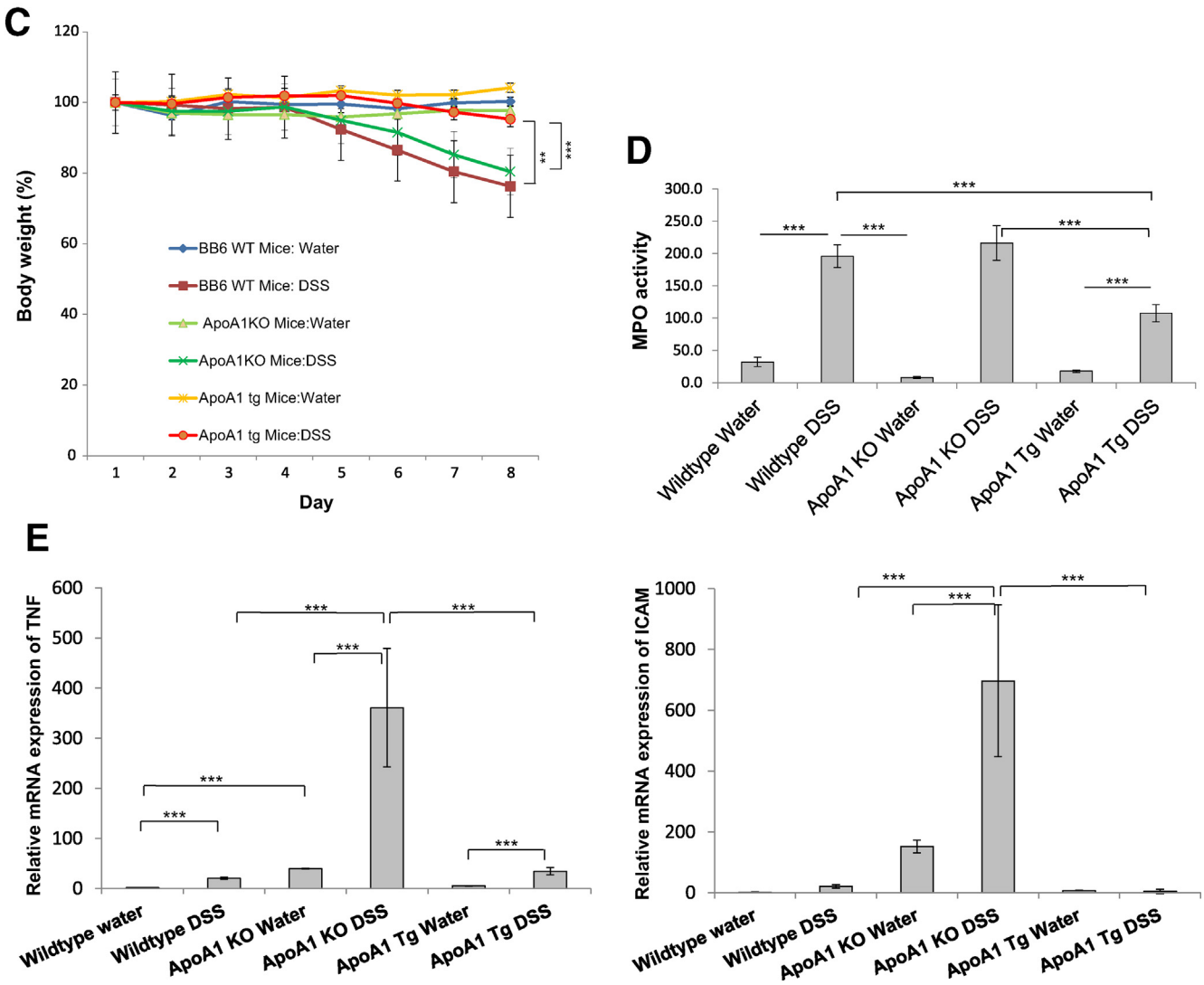

Figure 1. (*continued*).

demonstrated that HDL and apoA-I down-regulated the expression of proinflammatory cytokines via a NF-κB-dependent pathway. The mRNA expression of TNF, IL-8, and ICAM was quantified in T84 cells in the presence or absence of HDL. The T84 cells were incubated with 200 μg HDL for 18 hours and then stimulated with 25 ng/mL TNF for 3 hours. TNF significantly induced the mRNA expression of TNF, IL-8, and ICAM by factors of 178, 127, and 830, respectively, whereas HDL pretreatment significantly suppressed this expression by 59%, 31%, and 50%, respectively (Figure 3*A*). The suppressive effect of HDL on TNF-induced mRNA expression of TNF was concentration dependent, ranging from 20% in the presence of 50 μg/mL HDL to 60% in the presence of 200 μg/mL HDL (Figure 3*B*).

Lipid-free apoA-I mimicked these anti-inflammatory effects of HDL, pointing to an important role of apoA-I in this process. Incubation of T84 cells with 100 μg/mL apoA-I for 18 hours before the addition of 25 μg/mL TNF for 3 hours led to a decrease in TNF-induced mRNA expression of TNF, IL-8, and ICAM by 73%, 54%, and 51%, respectively (Figure 3*C*); the suppressive effect of apoA-I on the TNF-induced mRNA expression of TNF was concentration dependent (Figure 3*D*).

The down-regulation of proinflammatory cytokines by HDL and apoA-I occurred via a NF-κB-dependent pathway. Immunoblotting showed that when cells were pretreated with HDL for 18 hours and then stimulated for 3 hours with 25 ng/mL TNF, the phosphorylation of the IκB kinase complex (p-IKK), a process that precedes the translocation of NF-κB to the nucleus, was slightly decreased by HDL. Pretreatment of the cells with TNF increased p-IKK by 46%; however, this effect was reduced by 70% in the presence of HDL (Figure 3*E*).

Next, tests were performed to determine whether HDL suppresses TNF-induced NF-κB responsive promoter activity. The T84 cells were transiently transfected with luciferase constructs expressing an NF-κB responsive element.

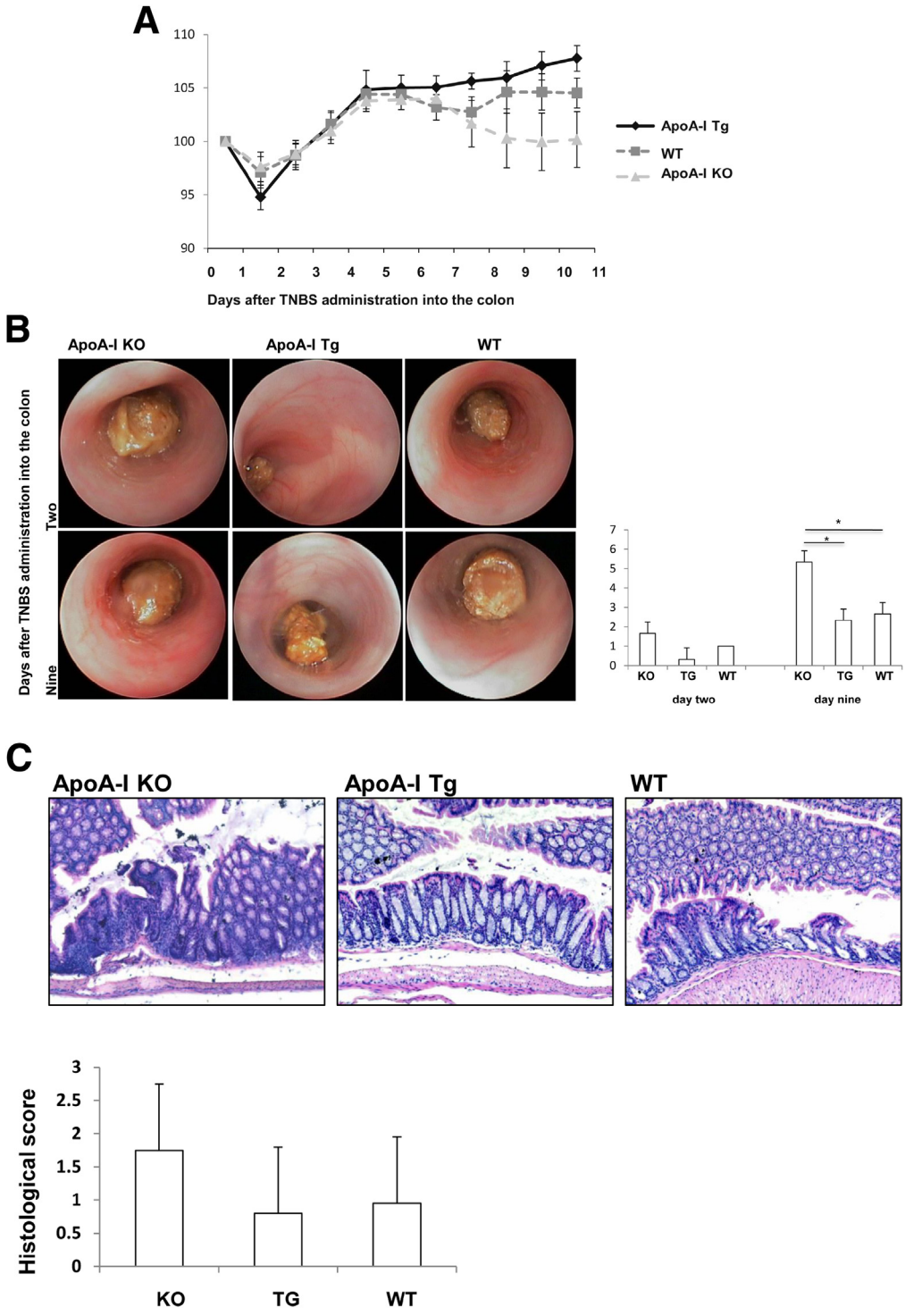

Figure 2. Intestinal inflammation is ameliorated in apolipoprotein A-I transgenic (apoA-I Tg) mice with colitis induced by 2,4,6-trinitrobenzenesulfonic acid (TNBS). (*A*) Percentage body weight loss showed an increase in body weight in apoA-I Tg mice compared with apoA-I knockout (KO) mice at days 9 and 10 after TNBS administration into the colon (± standard error of the mean [SEM], n = 5 each, **P* < .05). (*B*) Mini-endoscopy showed a clearly altered vascular pattern in apoA-I Tg mice receiving TNBS compared with both apoA-I KO and wild-type (WT) mice. Macroscopic mucosal damage was assessed by colonoscopy scoring (murine endoscopic index of colitis severity) (± standard deviation [SD], n = 5 each, **P* < .05). (*C*) H&E staining of sections from apoA-I KO mice receiving TNBS displayed barrier breakdown with infiltration. The total histologic score, calculated as the sum of the epithelium and infiltrate score, was plotted. Each bar represents the mean ± SD; n = 5.

After 24 hours, the cells were incubated with 100 μg/mL HDL for 18 hours and then 25 ng/mL TNF for 6 hours. HDL significantly inhibited NF-κB luciferase activity (by 26%). Treatment with TNF alone almost tripled luciferase activity, but preconditioning with HDL or lipid-free apoA-I significantly suppressed this effect (both by 50%; Figure 3*F*).

Nuclear extracts from T84 cells were subjected to EMSA. This showed that pretreatment of the T84 cells with HDL or apoA-I decreased TNF-induced binding of NF-κB to a 32P-labeled consensus NF-κB binding DNA sequence (Figure 3*G*).

High-Density Lipoprotein Induces Autophagy and Is Taken Up into Autophagosomes

Autophagy increases cell survival during periods of stress via catabolism of subcellular proteins, organelles, and

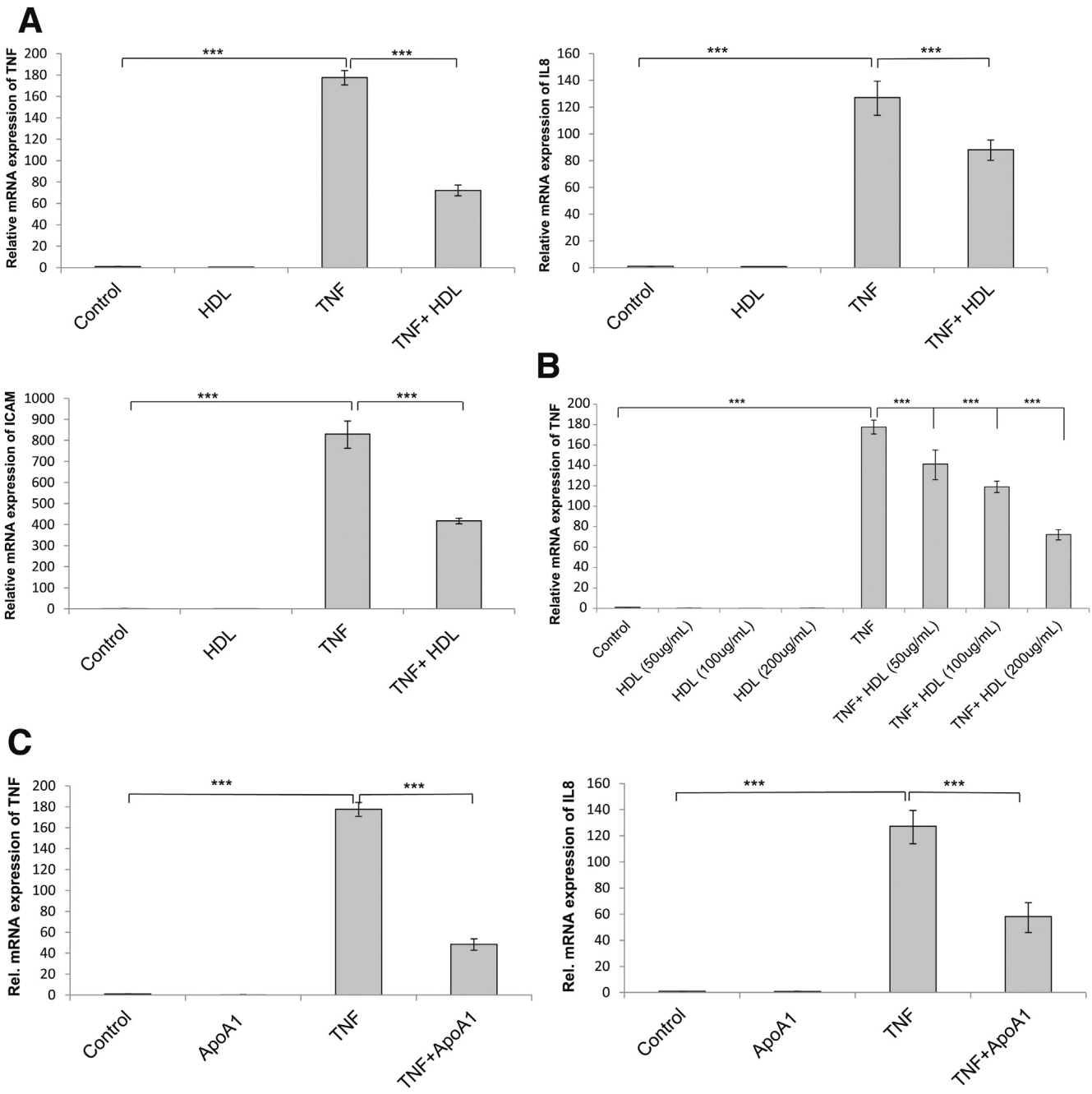

Figure 3. Anti-inflammatory effect of high-density lipoprotein (HDL) and apolipoprotein A-I (apoA-I) in vitro. (*A*) HDL suppressed tumor necrosis factor (TNF)-induced mRNA expression of TNF, interleukin-8 (IL-8), and intracellular adhesion molecule (ICAM). The mRNA expression of TNF, IL-8, and ICAM was quantified by reverse-transcriptase real-time polymerase chain reaction (RT-PCR) and normalized to actin. Results represent mean ± standard deviation (SD), n = 3, ***$P < .001$. (*B*) HDL suppressed TNF-induced mRNA expression of TNF in a concentration-dependent manner. The mRNA expression of TNF was quantified by RT-PCR and normalized to actin. Each bar represents the mean ± standard deviation (SD), n = 3, ***$P < .001$. (*C*) ApoA-I (similar to HDL) suppressed mRNA expression of TNF, IL-8, and ICAM. The mRNA expression of TNF, IL-8, and ICAM was quantified by RT-PCR and normalized to actin. The results represent the mean ± SD, n = 3, ***$P < .001$. (*D*) ApoA-I suppressed TNF-induced mRNA expression of TNF in a concentration-dependent manner. The mRNA expression of TNF was quantified by RT-PCR and normalized to actin. Each bar represents the mean ± SD, n = 3, ***$P < .001$. (*E*) HDL decreased the phosphorylation of IκB kinase (p-IKK). The p-IKK arbitrary units represent the ratio of p-IKK to actin normalized to the untreated controls. (*F*) HDL and apoA-I suppressed TNF-induced NF-κB-responsive promoter activity. *$P < .05$, ***$P < .001$. (*G*) HDL and apoA-I decreased the TNF-induced NF-κB DNA binding activity. The top arrow indicates the binding reaction of TNF to the NF-κB consensus, and the bottom arrow shows the supershift observed upon incubation of nuclear extracts with the anti-p65 antibody.

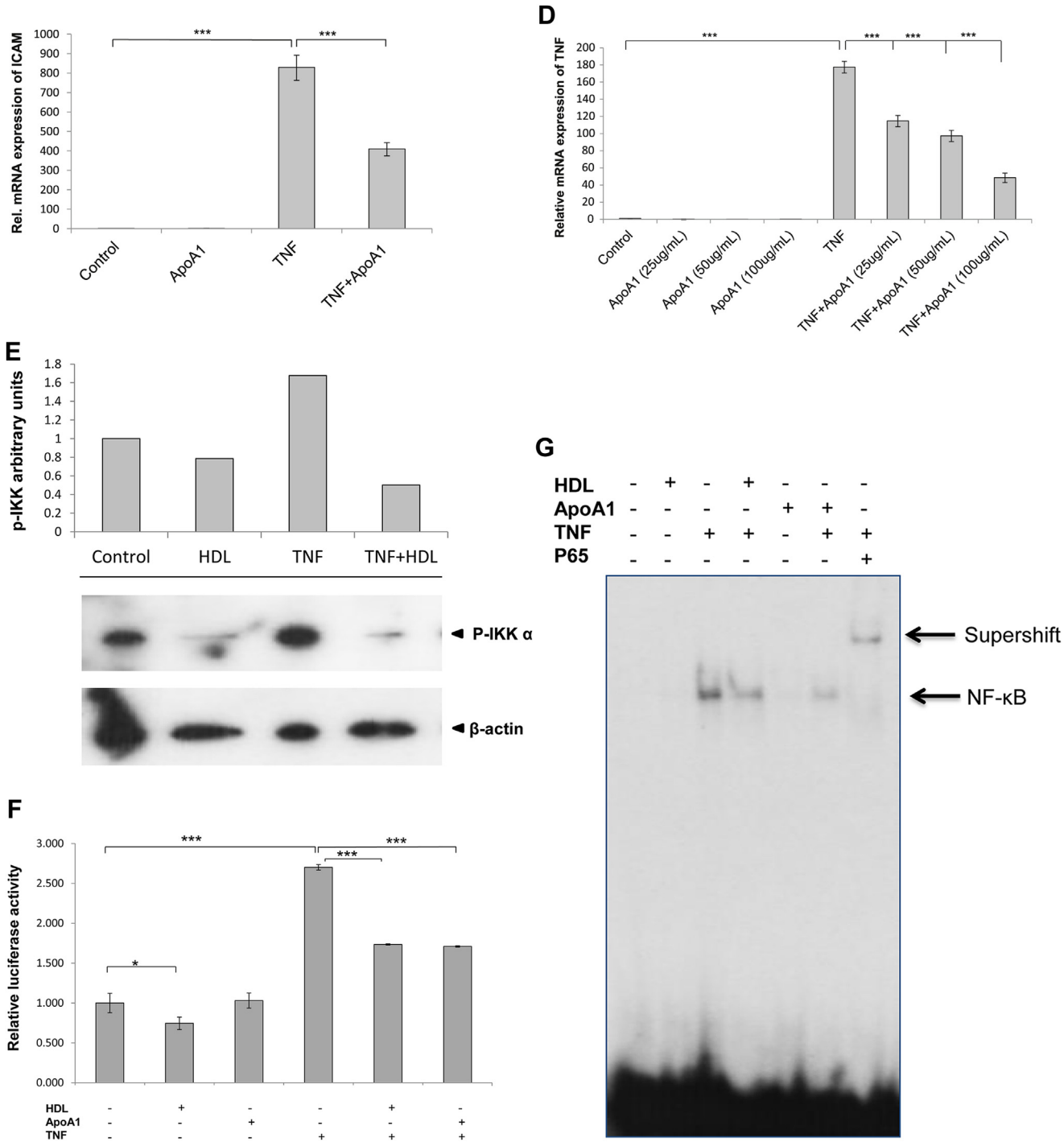

Figure 3. (*continued*).

cytoplasmic components that generate free fatty acids, amino acids, and nucleotides.[31–33] Autophagy is critically involved in regulating innate immune responses by providing a defence against intracellular microbial pathogens and mediating antigen presentation via MHC class-II molecules.[34,35] Dysfunctional autophagy is associated with defective bacterial handling, prolonged intracellular survival of pathogens, and uncontrolled inflammation. Autophagosomes are characterized by double membrane vesicles, the formation of which is mediated by autophagy proteins such as ATG12-ATG5-ATG16 and a microtubule associated protein light chain 3 (LC3). Increase in autophagy can be characterized by conversion of LC3-I to the phosphatidylethanolamine-conjugated form of LC3II that accumulates on autophagic vesicles.[36,37] Levels of autophagy proteins, such as ATG16L1 or IRGM, are significantly decreased in the intestine of Crohn's disease (CD) patients.[38] To date, three autophagy genes have been

confirmed as CD susceptibility genes, namely, ATG16L1, IRGM, and Leucine-rich repeat kinase 2 (LRRK2).

An uptake of HDL into vesicles that retrospectively appear to be autophagosomes has already been reported in 1992.[20] We therefore investigated whether the HDL/apoA-I mediated anti-inflammatory effect could be associated with autophagy. Incubation of T84 cells with HDL stimulated autophagy, as demonstrated by a significant increase in punctate staining for LC3. The T84 cells were treated with 0 or 100 μg/mL HDL for 18 hours, then fixed with 4% PFA, and stained for LC3 (green) or cell nuclei (4′,6-diamidino-2-phenylindole [DAPI, blue]). An increase in punctate staining—representing LC3 protein accumulation (ie, autophagosome formation)—was observed in the cells incubated with HDL (Figure 4*A*). Incubation of the T84 cells with HDL also led to increased conjugation of the cytosolic protein LC3I to the autophagosomal membrane-bound LC3II during autophagy. This was demonstrated by an increase in the LC3II:LC3I ratio after the incubation of T84 cells with increasing concentrations of HDL for 18 hours, confirmed by Western blot analysis and immunofluorescence analysis of whole cell protein extracts with anti-LC3 antibodies. The increase was concentration dependent, and LC3 II expression was maximum at 18 hours (Figure 4*B*).

The HDL-induced increase in LC3II was found to be mediated via inhibition of mTOR, a negative regulator of autophagy. T84 cells were treated with 50 μg HDL for 18 hours, and whole cell protein extracts were analyzed by Western blotting. Phosphorylation of mTOR decreased upon treatment with HDL by more than 50% (Figure 4*C*).

Electron microscopy revealed that HDL is taken up into autophagosomes. The T84 cells were incubated with 8 nm gold-labeled HDL for 18 hours and then fixed and embedded in Epon Araldite. Gold-labeled HDL was visible within vesicles resembling autophagosomes (the vesicles had typical characteristics of engulfed cytoplasmic materials and organelles and were found in close proximity to organelles

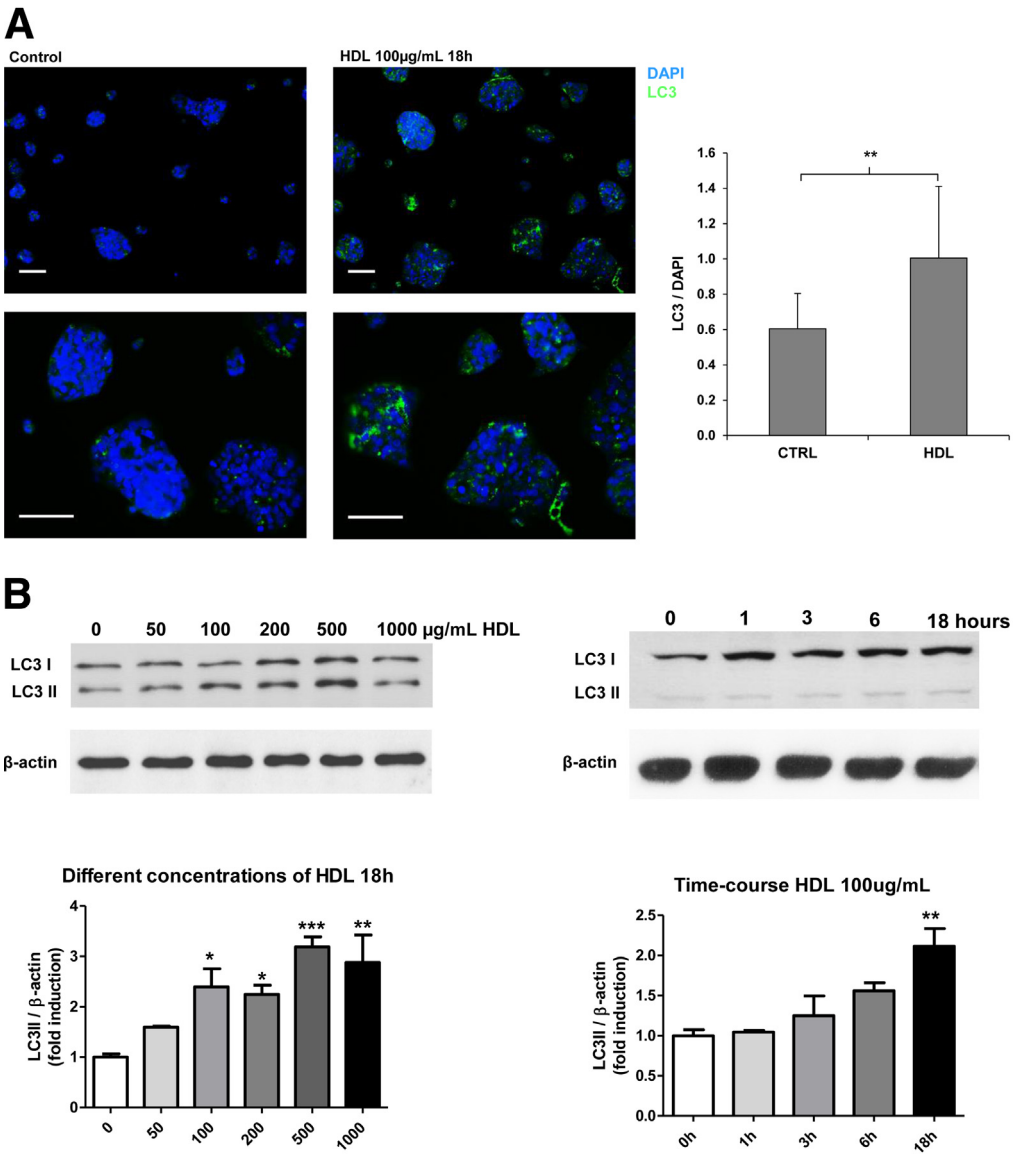

Figure 4. High-density lipoprotein (HDL) induces autophagy and is taken up into autophagosomes. (*A*) HDL increased autophagy, demonstrated by an increase in punctate staining for light chain 3 (LC3). The cells were stained for visualization of LC3 (green) or cell nuclei (DAPI [blue]). Scale bars: 25 μm. Representative data from one of four experiments is shown. (*B*) HDL induced an increase in conjugation of LC3II during autophagy. LC3 arbitrary units represent the ratio of LC3 to actin normalized to the untreated controls. (*C*) HDL decreased phosphorylation of mammalian target of rapamycin (p-mTOR), a negative regulator of autophagy. (*D*) HDL was taken up into autophagosomes. Electron microscopy shows autophagic uptake of gold-labeled HDL (*arrows*). (*E*) HDL was found to colocalize with LC3, confirming a possible autophagic uptake of HDL into cells, Scale bars: 25 μm.

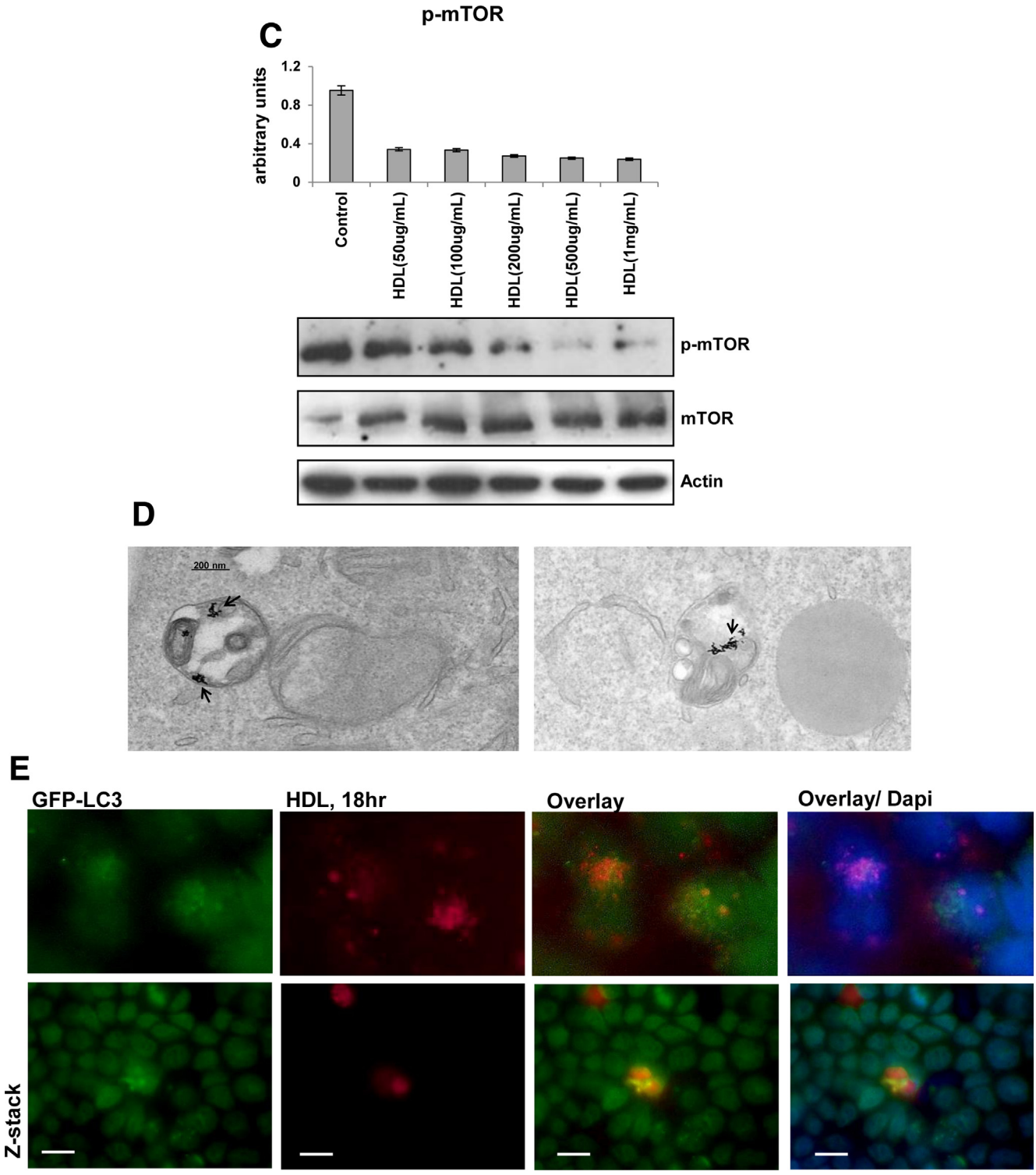

Figure 4. (*continued*).

that may represent lysosomes) (Figure 4*D*). Upon confocal immunofluorescence microscopy, HDL was found colocalized with LC3. The T84 cells were transduced with lentiviral constructs harboring GFP-LC3 and, after 24 hours, were incubated with fluorescently labeled HDL (Atto_655 HDL) for 18 hours. The cells were then fixed with 4% PFA, and the nuclei was stained with DAPI. Colocalization of HDL with LC3 was clearly demonstrated, supporting our conclusion of HDL uptake into autophagosomes of T84 cells (Figure 4*E*).

Autophagy is necessary for an HDL-mediated anti-inflammatory effect, which involves recruitment of p-IKK to

the autophagosome. The anti-inflammatory effect mediated by HDL was shown to be dependent on tubulin. The T84 cells were incubated with 5 μM colchicine (which binds tubulin and blocks its polymerization) followed by HDL 100 μg/mL for 18 hours and TNF 25 ng/mL for 3 hours. The addition of colchicine statistically significantly reversed by 19% ($P < .05$) the anti-inflammatory effect mediated by HDL on mRNA expression of TNF (Figure 5*A*).

The anti-inflammatory effect of HDL was also reversed after the inhibition of autophagy. The T84 cells were pretreated with the autophagy-specific class III phosphatidylinositol-3 (PI-3) kinase inhibitor 3-methyl adenine (3-MA) at a concentration of 10 nM or the PI-3 kinase inhibitor wortmannin at a concentration of 25 nM for 6 hours. Twenty-four hours after being transfected with luciferase constructs expressing NF-κB-responsive elements, the cells were incubated with 100 μg/mL HDL for 18 hours and then 25 ng/mL TNF for 6 hours. The ability of HDL to suppress TNF-induced NF-κB-responsive promoter activity, as analyzed by the use of a dual luciferase reporter assay, was decreased in the presence of 3-MA (by 26%) and wortmannin (33%) (Figure 5*B*).

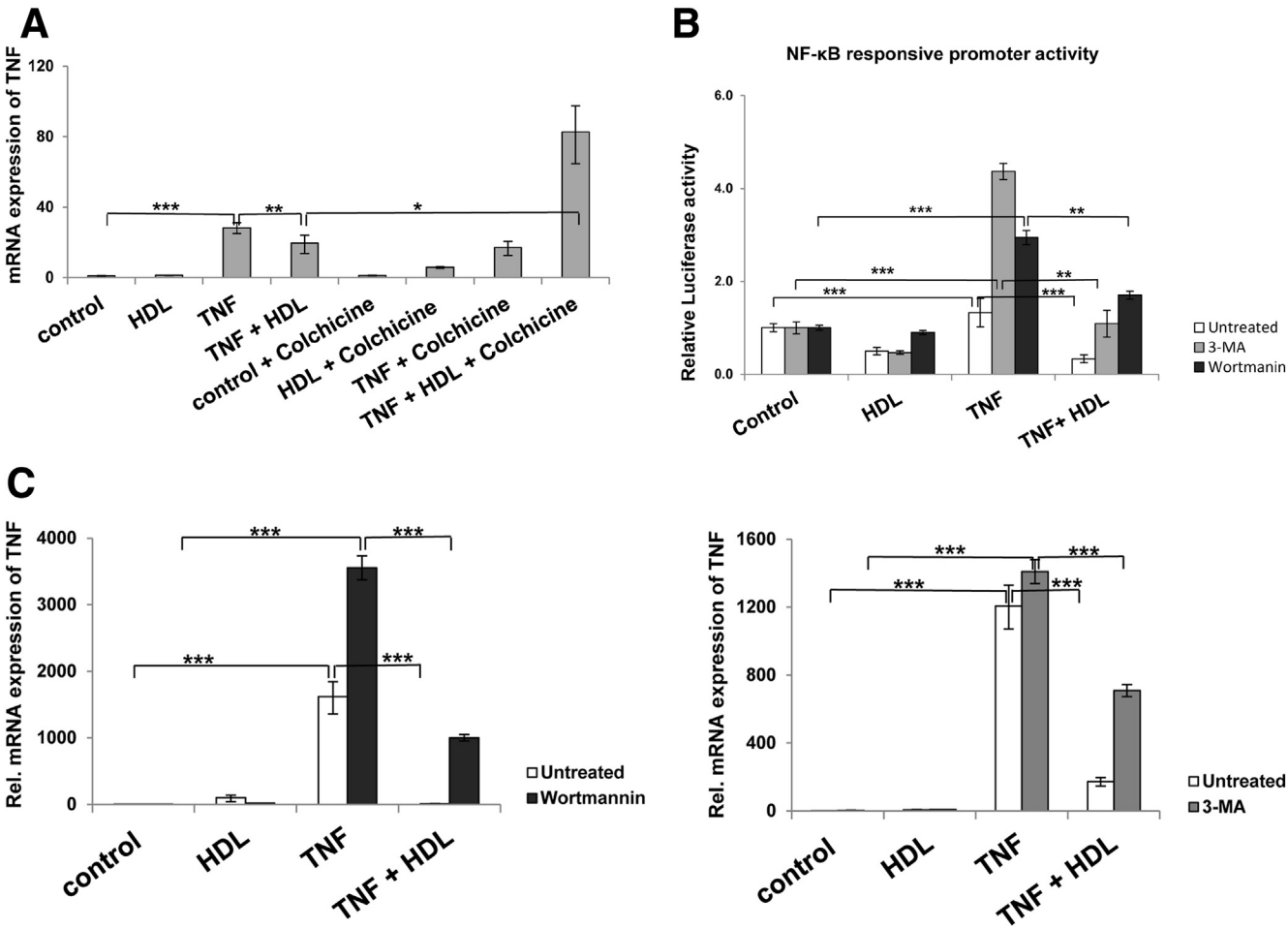

Figure 5. Autophagy is necessary for a high-density lipoprotein (HDL)-mediated anti-inflammatory effect, which involves the recruitment of phosphorylated IκB kinase (p-IKK) to the autophagosome. (*A*) The anti-inflammatory effect mediated by HDL on mRNA expression of TNF was tubulin dependent, as shown by incubation of T84 cells with colchicine (a tubulin blocker). The mRNA expression of TNF was quantified relative to actin. Each bar represents the mean ± standard deviation (SD), n = 3. (*B*) Inhibition of autophagy using the phosphatidylinositol-3 (PI-3) kinase inhibitor wortmannin and the autophagy-specific class III PI-3 kinase inhibitor 3-methyl adenine (3-MA) reversed the anti-inflammatory effect of HDL (as demonstrated by suppression of TNF-induced NF-κB-responsive promoter activity). Each bar represents the mean ± SD, n = 3. (*C*) Inhibition of autophagy (with wortmannin and 3-MA) reversed the anti-inflammatory effect of HDL (as demonstrated by suppression of TNF-induced mRNA expression of TNF). The mRNA expression of TNF was quantified relative to actin. Each bar represents the mean ± SD, n = 3. (*D*) The anti-inflammatory effect of HDL was decreased in the presence of the autophagosome fusion inhibitor bafilomycin A1. The mRNA expression of TNF was quantified relative to actin. Each bar represents the mean ± SD, n = 3. (*E*) The siRNA knockdown of the autophagy gene LC3 decreased the anti-inflammatory effect of HDL. The mRNA expression of LC3 and TNF was quantified relative to actin. Each bar represents the mean ± SD, n = 3. (*F*) In fibroblasts harboring the ATG16L1 mutation, the anti-inflammatory effect mediated by HDL was reduced. The mRNA expression of TNF was quantified relative to actin. Each bar represents the mean ± SD, n = 3. (*G*) HDL colocalizes with p-IKK and LC3 in T84 cells. Scale bars: 25 μm.

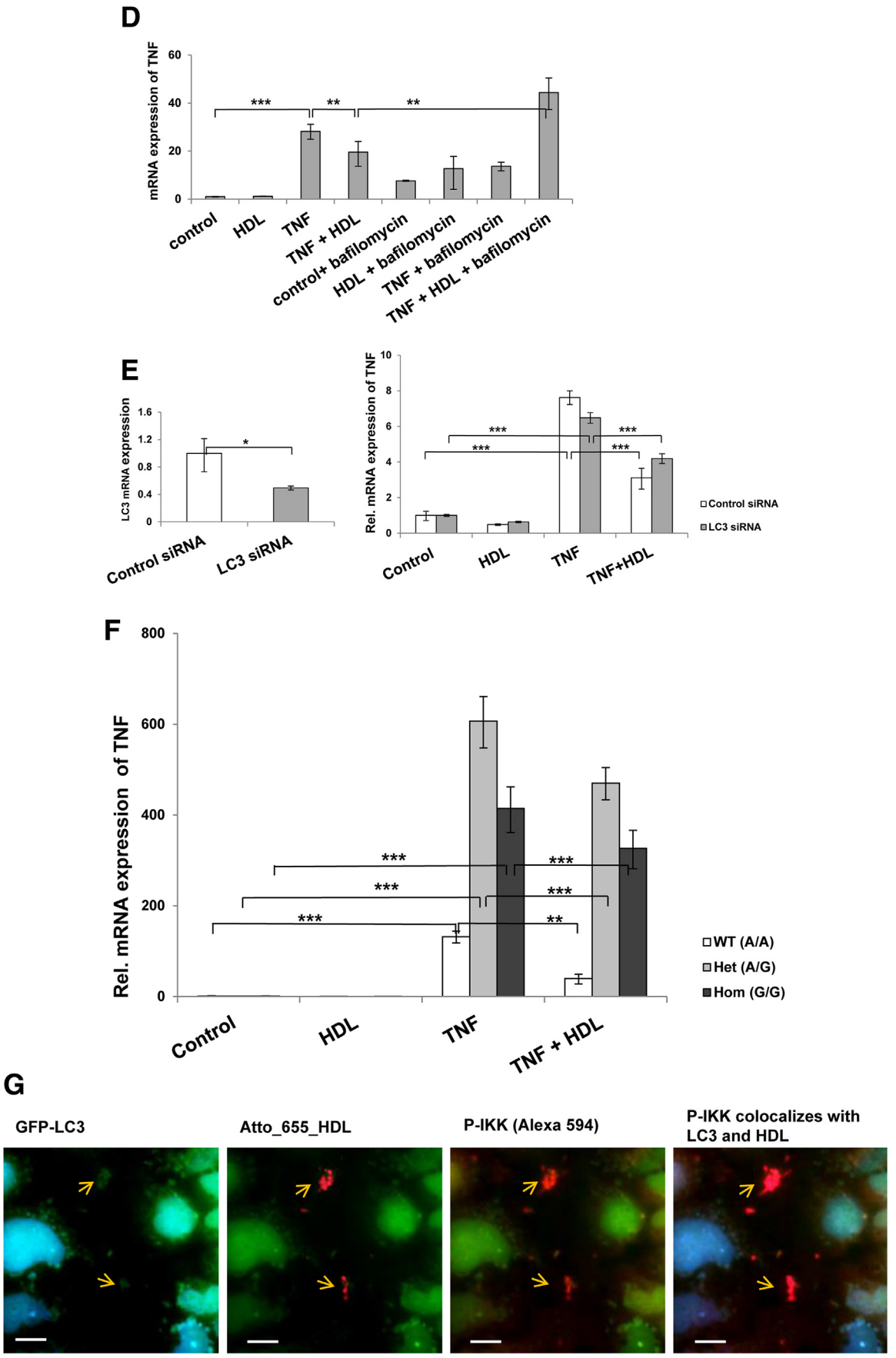

Figure 5. (*continued*).

In a similar experiment, after incubation for 6 hours with 3-MA and wortmannin, the cells were incubated with 100 μg/mL HDL for 18 hours followed by 25 ng/mL TNF for 3 hours. The ability of HDL to suppress the TNF-induced mRNA expression of TNF was significantly reduced in the presence of wortmannin and 3-MA (Figure 5*C*).

Further testing showed that the anti-inflammatory effect of HDL is decreased in the presence of the autophagosome fusion inhibitor bafilomycin A1. The T84 cells were pretreated with bafilomycin A1 100 nM (to inhibit autophagy) before the addition of HDL for 18 hours and subsequently 25 ng/mL TNF for 3 hours. Pretreatment with bafilomycin significantly decreased the ability of HDL to suppress TNF-induced mRNA expression of TNF by 31% (Figure 5*D*).

In addition, siRNA knock down of the autophagy gene LC3 decreased the anti-inflammatory effect of HDL. The T84 cells were transfected with 50 nM control siRNA or LC3 siRNA; 48 hours after transfection, the cells were incubated with 100 μg/mL HDL or 50 μg/mL apoA-I for 18 hours, before the incubation with 25 ng/mL TNF for 3 hours. A 33% decrease in LC3 expression was demonstrated (Figure 5*E*).

Genetic variants in autophagy genes ATG16L1 and IRGM1 have been shown to increase the susceptibility to CD.[39–41] Cells expressing the variant ATG16L1 protein were shown to have a defect in autophagy.[35,42–45] To investigate whether our finding is of relevance in humans, we isolated mucosal fibroblasts from CD patients with the ATG16L1 variant as well as WT patients. The anti-inflammatory effect mediated by HDL was significantly reduced in fibroblasts harboring the ATG16L1 mutation, which compromises autophagocytic activity. Human mucosa-derived fibroblasts were preconditioned with or without HDL for 18 hours, before the incubation with 25 ng/mL TNF for 3 hours. TNF stimulated mRNA expression of TNF more pronouncedly in fibroblasts with ATG16L1 mutations. The ability of HDL to suppress TNF-induced mRNA expression of TNF was significantly reduced by 44% and 12% in fibroblasts with homozygous and heterozygous ATG16L1 mutations as compared with control fibroblasts (Figure 5*F*). These results suggest that dysfunctional autophagy limits the anti-inflammatory functionality of HDL in human cells carrying the IBD-associated ATG16L1 variant.

To further investigate the role of HDL in the NF-κB pathway, whole cell protein from T84 cells was extracted and treated with HDL for 18 hours in the presence or absence of 25 ng/mL TNF. Immunoblotting showed that TNF increased p-IKK levels by 46%, but this effect was reduced by 70% in the presence of HDL (Figure 3*E*). To elucidate the relationship between HDL-induced autophagy and decreased NF-κB activation, a colocalization experiment was performed. The T84 cells were transfected with lentiviral constructs of GFP-LC3; Twenty-four hours after transfection, the cells were incubated with fluorescently labeled HDL (Atto_655 HDL) for 18 hours. The cells were fixed with 4% PFA and stained for p-IKK using Alexafluor 594 and for nuclei by using DAPI. Colocalization of LC3 with HDL and p-IKK was observed (Figure 5*G*), indicating that HDL might specifically recruit p-IKK to autophagosomes for degradation, resulting in a decreased inflammatory response via the prevention of further NF-κB activation and induction of cytokine expression.

These studies demonstrate that HDL and its major protein component apoA-I act in an anti-inflammatory manner via induction of autophagy and subsequent recruitment of p-IKK into autophagosomes. Traditionally, the many cytoprotective and anti-inflammatory functions of HDL have been related to the ability of HDL to regulate cellular cholesterol homeostasis by mediating cholesterol efflux[5,6,11] or to elicit signal transduction by the interaction with cell surface receptors such as scavenger receptor class B type I (SR-BI), sphingosine-1-phosphate receptors, or ectopic β-ATPase.[7,11] Our data suggest a third mechanism: endocytosis into intracellular organelles for neutralization of proinflammatory molecules. Endocytosis was previously identified as crucial for the antibiotic activity of HDL toward *Trypanosoma brucei*[46] but appears to be also relevant for the blockage of NF-kB signaling in epithelial cells. From the clinical perspective, our findings provide additional rationales to target or mimic[8] HDL for the treatment of inflammatory diseases such as IBD.

Conclusions

IBD patients of both genders display dyslipidemia with significantly lower HDL cholesterol. Because HDL is a negative acute phase reactant and because the intestine is the second most important site of HDL production, low HDL cholesterol has traditionally been interpreted to be the consequence of IBD. Because HDL exerts many anti-inflammatory activities on many cells including endothelial cells, pancreatic β-cells, and leukocytes, we hypothesized that HDL may also modulate intestinal inflammation.[11,47–50] We found evidence for anti-inflammatory effects of HDL and apoA-I in the intestine, both in vitro and in vivo.

The proinflammatory cytokine TNF alters the integrity of epithelial and endothelial cell barriers and is a key mediator of mucosal inflammation in both CD and ulcerative colitis. An increased concentration of TNF has been found in the blood, mucosa, and feces of CD patients.[51] In several animal models of IBD, genetic ablation or anti-TNF treatment result in amelioration of mucosal inflammation. Furthermore, infliximab, a monoclonal antibody against TNF has been effective in clinical management of IBD.[51,52–54] We therefore used TNF as a proinflammatory stimulator for our in vitro experiments. Preincubation of colon carcinoma T84 cells with HDL or apoA-I for 18 hours significantly suppressed TNF triggered mRNA expression of IL-8, ICAM, and TNF by inhibiting NF-κB promoter activity as measured by relative luciferase activity and NF-κB DNA binding activity by EMSA. These findings are very similar to those previously made in experiments with endothelial cells and vascular smooth muscle cells where HDL was also found to reduce cytokine production and adhesion molecule expression via inhibition of NF-κB.[55–58]

Importantly, the anti-inflammatory properties of HDL and apoA-I could be reproduced in an animal model of colitis. Upon DSS or TNBS treatment, the apoA-I KO phenotype exhibited a more severe intestinal inflammation compared with the WT mice, as indicated by increased

mucosal damage upon both colonoscopy and histology, shorter colon length, increased intestinal MPO activity, and mRNA expression of TNF and ICAM. Conversely, apoA-I Tg mice, which have elevated levels of HDL, were partially protected from DSS/TNBS-induced mucosal damage, as indicated by the less severe symptoms upon colonoscopy and less severe increase in MPO activity. The functional importance of the attenuated intestinal inflammation in apoA-I Tg mice is highlighted by the fact that WT and apoA-I KO mice but not apoA-I Tg mice lost body weight with DSS/TNBS treatment. These observations are in very good agreement with previous findings of Cuzzocrea et al,[57] who showed that administration of reconstituted HDL reduces intestinal inflammation in animals with splanchnic artery occlusion shock or colitis induced by dinitrobenzene sulfonic acid.

HDL and apoA-I have been increasingly recognized as a part of innate immune system for their ability to bind and neutralize the toxic effects of lipopolysaccharide, a bacterial product that can activate Toll-like receptors and thereby stimulate the secretion of cytokines.[59] This function may be of special importance in the control of barrier integrity, such as in the vascular endothelium and the intestinal epithelium.

Increased LC3-II is an indicator of preautophagosome formation. In our experiments, we observed increased processing of LC3 in the presence of HDL. This correlated with a decrease in phosphorylation of mTOR, a negative regulator of autophagy. Chemical inhibition of the autophagic pathway using wortmannin and 3-MA decreased the ability of HDL to decrease TNF-induced NF-κB responsive promoter activity as well as expression of TNF mRNA expression. Interestingly, pretreatment of T84 cells with bafilomycin A1, which inhibits the late stages of autophagosome fusion to lysosomes, also inhibited the suppressive effect mediated by HDL on TNF-induced mRNA expression of TNF. The intracellular transport of HDL seems to be tubulin mediated, as demonstrated by the reverse effect of HDL when T84 cells were incubated with colchicine, a tubulin blocker.

Whereas siRNA knockdown of LC3 significantly decreased the ability of HDL to suppress inflammation, siRNA knock down of the HDL receptors SRB1 and ABCA1 did not have any effect (data shown in Supplementary Figure 1). This observation correlates well with our studies in human fibroblasts harboring the ATG16L1 mutation. Further, we observed the uptake of gold-labeled HDL in autophagosomes, which clearly depicted engulfed organelles such as mitochondria and which were found in close proximity to lipid droplets. The autophagic uptake of HDL was confirmed by the colocalization of fluorescently labeled HDL with LC3 in colon carcinoma cells. In addition, we could colocalize p-IKK with LC3 and HDL, indicating that HDL might specifically recruit p-IKK to be degraded in autophagosomes.

These results give an initial indication that autophagy might regulate inflammatory pathways in intestinal cells and HDL might modulate inflammation via autophagy. In fact, apoL1, a minor component of HDL, has been shown to induce autophagy and modulate host immunity.[60–63]

Although Muller et al[65] have provided evidence that HDL may, in contrast, inhibit autophagy and endoplasmic reticulum stress induced by oxidized LDL in human microvascular endothelial cells, this effect cannot be generalized, taking into account the different cell model used and the fact that an increase in autophagy, especially selective autophagy, can have a positive effect in reducing cellular stress by the removal of specific stress factors enabling cell survival[64] but also can result in apoptosis and cellular death.[65]

Despite the complex crosstalk between autophagy, apoptosis, and endoplasmic reticulum stress, increasing evidence points to the association of dysfunctional autophagy with the pathogenesis of IBD. Genetic variation and dysfunction in the autophagy genes IRGM and ATG16L1 have been implicated in improper bacterial handling and abnormalities in Paneth cells.[39] Scharl et al[38] have published an interesting study showing that PTPN2 maintains intestinal barrier functions and limits the effects of proinflammatory cytokines by up-regulating autophagy. This study also shows that expression of autophagy proteins ATG16L1, IRGM, LC3, and ATG5-ATG12 are significantly decreased in the inflamed mucosa of CD patients. Future studies will be needed to determine whether the differences found in our preclinical models reflect the situation in macrophage and dendritic cell populations from patients with different ATG16L1 polymorphisms. The innate immune cells of patients with ATG16L1 polymorphisms will have to be studied for their response to HDL to take our findings into potential clinical application.

In summary, we report that HDL can decrease inflammation by suppressing TNF-induced NF-κB responses through the induction of autophagy. Chemical inhibition of autophagy as well as knockdown of autophagy genes decreased the ability of HDL to suppress inflammation in colon carcinoma cells. Immunofluorescence experiments also showed that HDL recruits p-IKK, a key component of the NF-κB pathway, to autophagosomes where they might be degraded, thereby decreasing NF-κB activation. Present day therapy of IBD consists of salicylates, corticosteroids, and immunosuppressants, most of which cause severe side effects. The clinical exploitation of HDL could be significant for the treatment of inflammatory diseases such as IBD.

References

1. Fisher EA, Feig JE, Hewing B, et al. High-density lipoprotein function, dysfunction, and reverse cholesterol transport. Arterioscler Thromb Vasc Biol 2012;32:2813–2820.
2. Lee-Rueckert M, Blanco-Vaca F, Kovanen PT, et al. The role of the gut in reverse cholesterol transport–focus on the enterocyte. Prog Lipid Res 2013;52:317–328.
3. Ono K. Current concept of reverse cholesterol transport and novel strategy for atheroprotection. J Cardiol 2012; 60:339–343.
4. Rosenson RS, Brewer HB Jr, Davidson WS, et al. Cholesterol efflux and atheroprotection: advancing the concept of reverse cholesterol transport. Circulation 2012;125:1905–1919.
5. Sorci-Thomas MG, Thomas MJ. High density lipoprotein biogenesis, cholesterol efflux, and immune cell function. Arterioscler Thromb Vasc Biol 2012;32:2561–2565.

6. Mineo C, Shaul PW. Novel biological functions of high-density lipoprotein cholesterol. Circ Res 2012;111:1079–1090.
7. Gordon SM, Davidson WS. Apolipoprotein A-I mimetics and high-density lipoprotein function. Curr Opin Endocrinol Diabetes Obes 2012;19:109–114.
8. Filippatos TD, Elisaf MS. High density lipoprotein and cardiovascular diseases. World J Cardiol 2013;5:210–214.
9. Patel PJ, Khera AV, Wilensky RL, et al. Anti-oxidative and cholesterol efflux capacities of high-density lipoprotein are reduced in ischaemic cardiomyopathy. Eur J Heart Fail 2013;15:1215–1219.
10. Annema W, von Eckardstein A. High-density lipoproteins. Circ J 2013;77:2432–2448.
11. Von Eckardstein A, Sibler RA. Possible contributions of lipoproteins and cholesterol to the pathogenesis of diabetes mellitus type 2. Curr Opin Lipidol 2011;22:26–32.
12. Demarin V, Lisak M, Morovic S, et al. Low high-density lipoprotein cholesterol as the possible risk factor for stroke. Acta Clin Croat 2010;49:429–439.
13. Morton J, Ng MK, Chalmers J, et al. The association of high-density lipoprotein cholesterol with cancer incidence in type ii diabetes: a case of reverse causality? Cancer Epidemiol Biomarkers Prev 2013;22:1628–1633.
14. Jafri H, Alsheikh-Ali AA, Karas RH. Baseline and on-treatment high-density lipoprotein cholesterol and the risk of cancer in randomized controlled trials of lipid-altering therapy. J Am Coll Cardiol 2010;55:2846–2854.
15. Yaari S, Goldbourt, Even-Zohar S, Neufeld HN. Associations of serum high density lipoprotein and total cholesterol with total, cardiovascular, and cancer mortality in a 7-year prospective study of 10 000 men. Lancet 1981;1:1011–1015.
16. Colin S, Briand O, Touche V, et al. Activation of intestinal peroxisome proliferator-activated receptor-alpha increases high-density lipoprotein production. Eur Heart J 2013;34:2566–2574.
17. Lutton C, Champarnaud G. Cholesterol synthesis and high density lipoprotein uptake are regulated independently in rat small intestinal epithelium. Gut 1994;35:343–346.
18. Sappati Biyyani RS, Putka BS, Mullen KD. Dyslipidemia and lipoprotein profiles in patients with inflammatory bowel disease. J Clin Lipidol 2010;4:478–482.
19. Williams HR, Willsmore JD, Cox IJ, et al. Serum metaboling profiling in inflammatory bowel disease. Dig Dis Sci 2012;57:2157–2165.
20. Rogler G, Herold G, Fahr C, et al. High-density lipoprotein 3 retroendocytosis: a new lipoprotein pathway in the enterocyte (Caco-2). Gastroenterology 1992;103:469–480.
21. Fielding CJ, Havel RJ, Todd KM, et al. Effects of dietary cholesterol and fat saturation on plasma lipoproteins in an ethnically diverse population of healthy young men. J Clin Invest 1995;95:611–618.
22. Von Eckardstein A, Funke H, Walter M, et al. Structural analysis of human apolipoprotein A-I variants. Amino acid substitutions are nonrandomly distributed throughout the apolipoprotein A-I primary structure. J Biol Chem 1990;265:8610–8617.
23. Saborowski M, Kullak-Ublick GA, Eloranta JJ. The human organic cation transporter-1 gene is transactivated by hepatocyte nuclear factor-4α. J Pharmacol Exp Ther 2006;317:778–785.
24. Obermeier F, Kojouharoff G, Hans W, et al. Interferon-gamma (IFN-gamma)- and tumour necrosis factor (TNF)-induced nitric oxide as toxic effector molecule in chronic dextran sulphate sodium (DSS)-induced colitis in mice. Clin Exp Immunol 1999;116:238–245.
25. Wirtz S, Neufert C, Weigmann B, et al. Chemically induced mouse models of intestinal inflammation. Nat Protoc 2007;2:541–546.
26. Becker C, Fantini MC, Neurath MF. High resolution colonoscopy in live mice. Nat Protoc 2006;1:2900–2904.
27. Huang EH, Carter JJ, Whelan RL, et al. Colonoscopy in mice. Surg Endosc 2002;16:22–24.
28. Becker C, Fantini MC, Neurath MF. High resolution colonoscopy in live mice. Nat Protoc 2007;1:2900–2904.
29. Steidler L, Hans W, Schotte L, et al. Treatment of murine colitis by *Lactococcus lactis* secreting interleukin-10. Science 2000;289:1352–1355.
30. Frens G. Controlled nucleation for the regulation of the particle size in monodisperse gold suspensions. Nature Phys Sci 1973;241:20–22.
31. Choi AM, Ryter SW, Levine B. Autophagy in human health and disease. N Engl J Med 2013;368:651–662.
32. Nys K, Agostinis P, Vermeire S. Autophagy: a new target or an old strategy for the treatment of Crohn's disease? Nat Rev Gastroenterol Hepatol 2013;10:395–401.
33. Deretic V, Saitoh T, Akira S. Autophagy in infection, inflammation and immunity. Nat Rev Immunol 2013;13:722–737.
34. Cooney R, Baker J, Brain O, et al. NOD2 stimulation induces autophagy in dendritic cells influencing bacterial handling and antigen presentation. Nat Med 2010;16:90–97.
35. Travassos LH, Carneiro LA, Ramjeet M, et al. Nod1 and Nod2 direct autophagy by recruiting ATG16L1 to the plasma membrane at the site of bacterial entry. Nat Immunol 2010;11:55–62.
36. Kabeya Y, Mizushima N, Ueno T, et al. LC3, a mammalian homologue of yeast Apg8p, is localized in autophagosome membranes after processing. EMBO J 2000;19:5720–5728.
37. Tanida I, Minematsu-Ikeguchi N, Ueno T, Kominami E. Lysosomal turnover, but not a cellular level, of endogenous LC3 is a marker for autophagy. Autophagy 2005;1:84–91.
38. Scharl M, Wojtal KA, Becker HM, et al. Protein tyrosine phosphatase nonreceptor type 2 regulates autophagosome formation in human intestinal cells. Inflammatory Bowel Diseases 2012;18:1287–1302.
39. Hampe J, Franke A, Rosenstiel P, et al. A genome-wide association scan of nonsynonymous SNPs identifies a susceptibility variant for Crohn disease in ATG16L1. Nat Genet 2007;39:207–211.
40. Rioux JD, Xavier RJ, Taylor KD, et al. Genome-wide association study identifies new susceptibility loci for Crohn disease and implicates autophagy in disease pathogenesis. Nat Genet 2007;39:596–604.

41. Raelson JV, Little RD, Ruether A, et al. Genome-wide association study for Crohn's disease in the Quebec Founder Population identifies multiple validated disease loci. Proc Natl Acad Sci USA 2007;104:14747–14752.
42. Klionsky DJ. Crohn's disease, autophagy, and the Paneth cell. N Engl J Med 2009;360:1785–1786.
43. Yano T, Kurata S. An unexpected twist for autophagy in Crohn's disease. Nat Immunol 2009;10:134–136.
44. Cadwell K, Liu JY, Brown SL, et al. A key role for autophagy and the autophagy gene Atg16l1 in mouse and human intestinal Paneth cells. Nature 2008;456:259–263.
45. Saitoh T, Fujita N, Jang MH, et al. Loss of the autophagy protein Atg16L1 enhances endotoxin-induced IL-1β production. Nature 2008;456:264–268.
46. Stephens NA, Kieft R, Macleod A, Hajduk SL. Trypanosome resistance to human innate immunity: targeting Achilles' heel. Trends Parsitol 2012;28:539–545.
47. Gordon SM, Hofmann S, Askew DS, Davidson WS. High density lipoprotein: it's not just about lipid transport anymore. Trends Endocrinol Metab 2011;22:9–15.
48. Besler C, Lüscher TF, Landmesser U. Molecular mechanisms of vascular effects of high-density lipoprotein: alterations in cardiovascular disease. EMBO Mol Med 2012;4:251–268.
49. Murphy AJ, Westerterp M, Yvan-Charvet L, Tall AR. Antiatherogenic mechanisms of high density lipoprotein: effects on myeloid cells. Biochim Biophys Acta 2012; 1821:513–521.
50. Drew BG, Rye K-A, Duffy SJ, et al. The emerging role of HDL in glucose metabolism. Nat Rev Endocrinol 2012; 8:237–245.
51. Van Deventer SJH. Targeting TNF alpha as a key cytokine in the inflammatory processes of Crohn's disease—the mechanisms of action of infliximab. Aliment Pharmacol Ther 1999;13(Suppl 4):3–8, 38.
52. Kontoyiannis D, Pasparakis M, Pizarro TT, et al. Impaired on/off regulation of TNF biosynthesis in mice lacking TNF AU-rich elements: implications for joint and gut-associated immunopathologies. Immunity 1999;10: 387–398.
53. Targan SR, Hanauer SB, van Deventer SJH, et al. A short-term study of chimeric monoclonal antibody cA2 to tumor necrosis factor α for Crohn's disease. N Engl J Med 1997;337:1029–1036.
54. Lichtenstein GR, Abreu MT, Cohen R, et al. American Gastroenterological Association Institute technical review on corticosteroids, immunomodulators, and infliximab in inflammatory bowel disease. Gastroenterology 2006;130:940–987.
55. Besler C, Heinrich K, Rohrer L, et al. Mechanisms underlying adverse effects of HDL on eNOS-activating pathways in patients with coronary artery disease. J Clin Invest 2011;121:2693–2708.
56. Robbesyn F, Garcia V, Auge N, et al. HDL counterbalance the proinflammatory effect of oxidized LDL by inhibiting intracellular reactive oxygen species rise, proteasome activation, and subsequent NF-κB activation in smooth muscle cells. FASEB J 2003;17:743–745.
57. Cuzzocrea S, Dugo L, Patel NS, et al. High-density lipoproteins reduce the intestinal damage associated with ischemia/reperfusion and colitis. Shock 2004;21: 342–351.
58. Di Bartolo BA, Nicholls SJ, Bao S, et al. The apolipoprotein A-I mimetic peptide ETC-642 exhibits antiinflammatory properties that are comparable to high density lipoproteins. Atherosclerosis 2011;217: 395–400.
59. Wang Y, Zhu X, Wu G, et al. Effect of lipid-bound apoA-I cysteine mutants on lipopolysaccharide-induced endotoxemia in mice. J Lipid Res 2008;49: 1640–1645.
60. Vanhollebeke B, Pays E. The trypanolytic factor of human serum: many ways to enter the parasite, a single way to kill. Mol Microbiol 2010;76:806–814.
61. Pays E, Vanhollebeke B. Human innate immunity against African trypanosomes. Curr Opin Immunol 2009;21: 493–498.
62. Pérez-Morga D, Vanhollebeke B, Paturiaux-Hanocq F, et al. Apolipoprotein L-I promotes trypanosome lysis by forming pores in lysosomal membranes. Science 2005; 309:469–472.
63. Wan G, Zhaorigetu S, Liu Z, et al. Apolipoprotein L1, a novel Bcl-2 homology domain 3-only lipid-binding protein, induces autophagic cell death. J Biol Chem 2008; 283:21540–21549.
64. Mizumura K, Choi AM, Ryter SW. Emerging role of selective autophagy in human diseases. Front Pharmacol 2014;5:244.
65. Muller C, Salvayre R, Nègre-Salvayre A, et al. HDLs inhibit endoplasmic reticulum stress and autophagic response induced by oxidized LDLs. Cell Death Differ 2011;18:817–828.

Received June 16, 2014. Accepted December 12, 2014.

Correspondence
Address correspondence to: Gerhard Rogler, MD, PhD, Division of Gastroenterology and Hepatology, University Hospital Zurich, Rämistrasse 100, 8091 Zurich, Switzerland. e-mail: gerhard.rogler@usz.ch; fax: +41-0-44-255-9497.

Conflicts of interest
The authors disclose no conflicts.

Funding
This study was funded by research grants from the Swiss National Science Foundation (Grant 320030_120463), and the Zurich Center for Integrative Human Physiology (ZIHP).

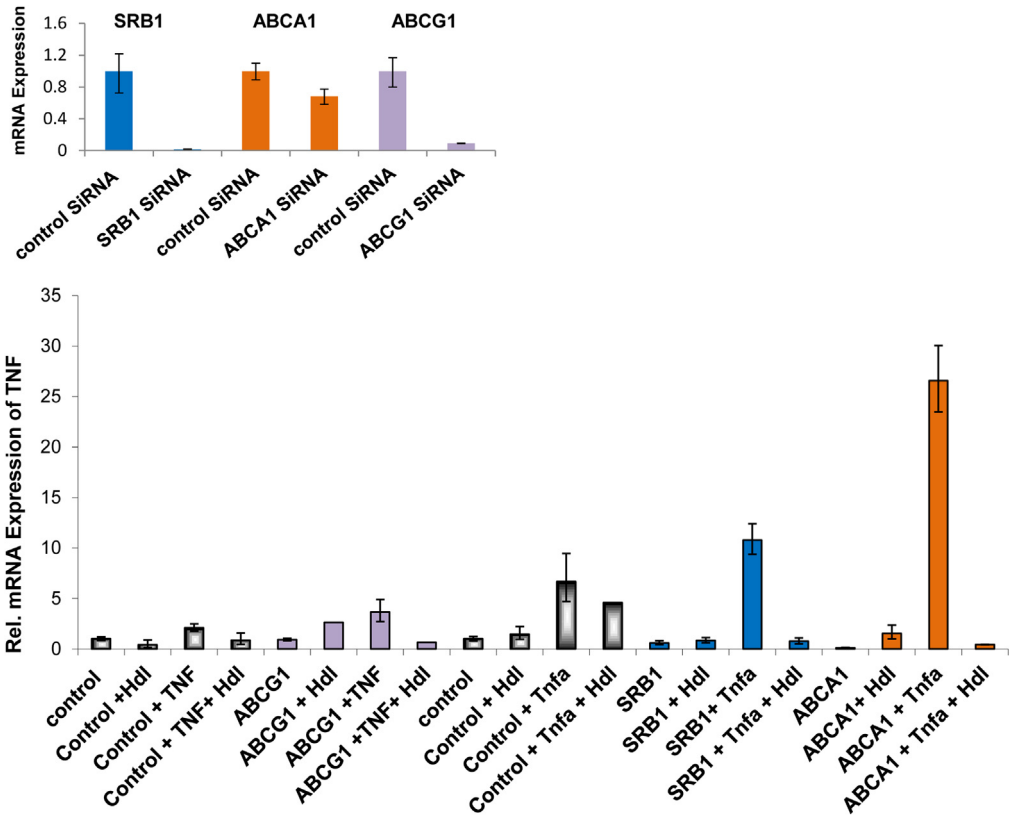

Supplementary Figure 1. The siRNA mediated knock down of the HDL receptors SRB1 and ABCA1 as well as ABCG1 did not have a significant effect on HDL mediated suppression of TNF mRNA induction by TNF stimulation. The mRNA expression of TNF, SRB1, ABCA1, and ABCG1 was quantified relative to actin. Each bar represents the mean ± SD, n = 3.